



Low distortion, continuously tunable, positive and negative time delays by slow and fast light using stimulated Brillouin scattering

Zhimin Shi^a, Aaron Schweinsberg^a, Joseph E. Vornehm Jr.^a, M. Alejandrina Martínez Gámez^b, Robert W. Boyd^{a,*}

^a The Institute of Optics, University of Rochester, Rochester, NY 14627, USA

^b Centro de Investigaciones en Óptica, Loma del Bosque 115, Col. Lomas del Campestre, León 37150, Gto., Mexico

ARTICLE INFO

Article history:

Received 21 March 2010
Received in revised form 4 August 2010
Accepted 6 August 2010
Available online 7 August 2010
Communicated by R. Wu

Keywords:

Slow light
Group delay
Stimulated Brillouin scattering

ABSTRACT

We demonstrate a single optical timing module that can provide both tunable delay and advancement with low distortion using a reconfigurable gain medium based on stimulated Brillouin scattering. Dual-stage intensity modulation method is used to achieve optimized gain profiles for both slow- and fast-light operation. Using 6.5 ns Gaussian pulses, we demonstrate a continuous temporal adjustment from a fractional advancement of 0.31 to a fractional delay of 0.82, giving more than a full pulse width of total tunability.

© 2010 Elsevier B.V. All rights reserved.

1. Introduction

Slow and fast light [1] have promising applications in telecommunication systems and all-optical signal processing. Among various slow-light processes [2–5], stimulated Brillouin scattering (SBS) [6,7] is a convenient process to achieve tunable delays in an optical fiber. Many techniques have been proposed to improve aspects of an SBS-based slow-light delay element, such as its operating signal bandwidth [8–11] and maximal achievable fractional delay [13–18]. Fast light has also been investigated in SBS systems [19–22], but most fast-light modules reported so far have very limited fractional advancement.

In practice, the temporal position of an optical signal train can experience random delay or advancement as compared to a reference clock. Thus, for applications such as jitter correction and data resynchronization, one would naturally desire a single timing element that could provide both positive and negative temporal adjustment. However, most demonstrated slow-light devices cannot be reconfigured easily to work in the fast-light regime, and vice-versa. It has been shown recently [19] that one can achieve tunable delay and advancement by adjusting the separation between two Lorentzian gain lines. However, in the process of tuning the separation, both the gain and group index profiles can become highly frequency dependent over the signal bandwidth. This leads

to significant pulse distortion and degradation of the signal fidelity, which becomes impractical for real applications.

2. Theory

In this work, we construct a continuously tunable SBS timing element that can achieve both positive and negative delays with a total tuning range of more than one pulse width with low distortion for both delay and advancement. For a single-frequency continuous-wave pump field, the SBS-induced complex refractive index near the Stokes frequency ν_0 can be approximated by a Lorentzian function as follows:

$$\tilde{n}(\nu) = n_{\text{bg}} + \frac{cg}{4\pi\nu_0} \frac{\gamma}{\nu - \nu_0 + i\gamma}, \quad (1)$$

where n_{bg} is the background index of refraction, c is the speed of light in vacuum, and g and γ are the peak gain coefficient and the SBS linewidth, respectively. The real part of \tilde{n} has a large swing in the vicinity of the resonance, resulting in slow and fast light in the center and wings of the resonance, respectively. The general principle of switching our device between slow- and fast-light operations is to reshape the SBS-induced gain profile by modulating the pump field differently, so that the signal spectrum lies either within the center region of a single gain feature or within the transparent window between two separated gain features.

Under many circumstances, the primary figure of merit of slow-light delay devices is the maximum achievable fractional delay $\overline{\Delta T}_{\text{max}}$ [12], also known as the delay-bandwidth product [23]. In this work, we define the fractional delay as $\overline{\Delta T} \equiv \Delta T/\tau_p$, where

* Corresponding author.

E-mail addresses: zshi@optics.rochester.edu (Z. Shi), boyd@optics.rochester.edu (R.W. Boyd).

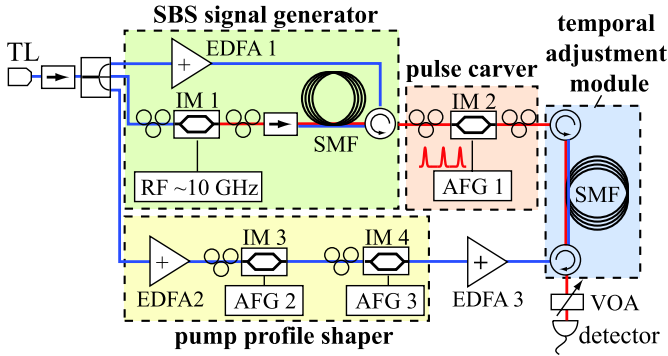


Fig. 1. (Color online.) Schematic diagram of a continuously tunable optical timing element based on stimulated Brillouin scattering that is capable of producing both positive and negative time delays. TL: tunable laser; IM: intensity modulator; AFG: arbitrary function generator; SMF: single-mode fiber; EDFA: erbium doped fiber amplifier; VOA: variable optical attenuator.

ΔT is the absolute delay of the peak position of the pulse as compared to that of a reference, and τ_p is the full width at half maximum (FWHM) of the input pulse.

In practice, ΔT_{\max} is often limited by the maximum distortion or change in power level that a signal is allowed to acquire in passing through a slow-light material [24]. To achieve large fractional delay and advancement to reach a total tuning range larger than a pulse width, we choose two optimized gain profiles with low distortion for slow- and fast-light operation. In this manner, signal distortion is well controlled through the entire tuning process. Tunable delay and advancement are then achieved by controlling the pump power.

In the slow light regime, we use multiple closely spaced gain lines for slow-light operation [14,15,25], and we optimize the spacing and the relative strength to form a broad, flat-top gain profile. One can also extend this concept to the use of a continuous pump spectrum to achieve a gain profile as broad as tens of gigahertz [26].

For fast-light operation, we use two separated gain features, which leaves a transparent, fast-light window in between. Note that the maximum achievable fractional advancement of such a separated double gain medium is determined by factors that can be different from those for a slow-light medium [24]. First, since the signal spectrum sits between two gain features, the wing regions of the signal spectrum gets amplified more than the center. This leads to spectrum broadening, and consequently the output pulses become narrower in the time domain. Furthermore, residual frequency components due to optical noise in the input signal or spontaneous emission from the gain medium that fall on the two gain peaks get amplified much more strongly than the main spectrum of the signal. Such amplified noise can form a beating pattern in the time domain, which leads to pulse distortion and inter-symbol interference [27]. Thus, instead of the maximum pump power the system can provide, this noise constraint determines the maximum continuous-wave (CW) gain the system can have at the two gain peaks, and hence further limits the maximum advancement that such a fast-light element can produce. Given such a limit, we use two separated, flat-top gain profiles to further increase the fractional advancement. In specific, each flat-top gain profile is created using three closely spaced gain lines.

3. Experimental demonstration

The schematic diagram of our experiment is plotted in Fig. 1. We start with a stable laser source (Koshin LS-601A) at a frequency ν_0 near 1550 nm, and we modulate the field using a sinusoidally driven Mach-Zehnder (MZ) intensity modulator (IM 1 in Fig. 1),

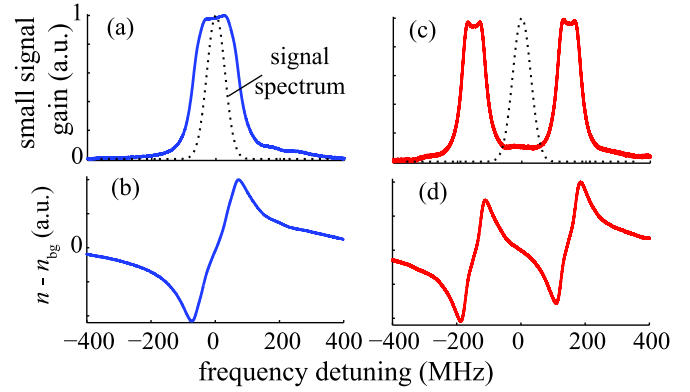


Fig. 2. (Color online.) Measured small signal gain and calculated induced refractive index change as functions of frequency detuning for slow light [(a) and (b)] and fast light [(c) and (d)] configurations. The black dotted lines in (a) and (c) show the power spectrum of Gaussian pulses with FWHM of 6.5 ns.

which is biased for minimum DC transmission. The modulator creates two frequency sidebands, $\nu_0 \pm \Omega_B$, where $\Omega_B \approx 10.6$ GHz is the SBS Stokes shift frequency of our single-mode fiber (SMF). The modulated field then propagates through 6 km of SMF with a strong counter-propagating pump field at ν_0 . The SBS process amplifies the component at the Stokes frequency $\nu_0 - \Omega_B$ and attenuates the anti-Stokes frequency $\nu_0 + \Omega_B$. The optical field after this SBS purification stage is checked with an optical spectrum analyzer, and the power of the Stokes field at $\nu_0 - \Omega_B$ is 20 dB higher than those at ν_0 and $\nu_0 + \Omega_B$. A second MZ intensity modulator (IM 2) is then used to carve out a train of Gaussian pulses with FWHM width $\tau_{\text{FWHM}} = 6.5$ ns before the signal is sent into the SBS temporal adjustment module.

A two-stage pump modulation is used to reconfigure the two optimized SBS gain profiles between slow- and fast-light operations. We use one sinusoidally driven MZ intensity modulator (IM 3 in Fig. 1) to create three closely spaced frequency lines which lead to a single flattened gain feature approximately 80 MHz wide [15]. Note that one can use a more complicated modulation method [16,17] to create more lines and to form a broader gain feature. A second MZ intensity modulator (IM 4) is used to configure the final gain profile for slow- or fast-light operation. The modulator is always biased at minimum DC transmission, and it is sinusoidally modulated at frequency f_s . This setting splits the gain feature produced by IM 3 into two, separated by $2f_s$ from each other. For slow-light operation, the optimum value of f_s is approximately 34 MHz, and the two gain features are partially overlapped to form a broad, flat-top gain feature [see Fig. 2(a)]. For fast-light operation, the optimum value for f_s is approximately 148 MHz. The resulting two flat-top gain profiles are separated enough to leave a transparent fast-light window in between for our signal [see Fig. 2(c)], but they are also close enough that signal experiences a significant fast-light effect.

To illustrate the low-distortion advantage of our optimized gain profiles for the slow- and fast-light operations, we performed a numerical calculation of the width of the output pulse as the delay is increased by tuning up the pump power. Since the temporal shape of the output pulse can be irregular, such as having multiple lobes, it is more accurate to describe the temporal width of the pulse using its root-mean-square (RMS) width τ_{rms} as follows:

$$\tau_{\text{rms}} \equiv \sqrt{\langle t^2 \rangle - \langle t \rangle^2}, \quad (2)$$

where

$$\langle t \rangle = \frac{\int t |A(t)|^2 dt}{\int |A(t)|^2 dt}, \quad (3)$$

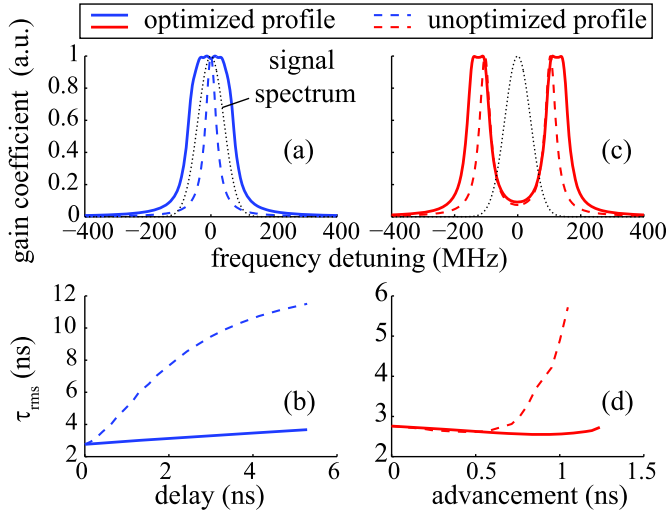


Fig. 3. (Color online.) Calculated optimized and un-optimized gain profiles as functions of frequency detuning for slow light (a) and fast light (c) configurations, and the RMS width of the output pulse for different gain profiles as functions of peak delay for slow light (b) or advancement for fast light (d) configuration.

$$\langle t^2 \rangle = \frac{\int t^2 |A(t)|^2 dt}{\int |A(t)|^2 dt}, \quad (4)$$

and where $A(t)$ is the amplitude of the pulse. The temporal RMS width of the input Gaussian pulses is $\tau_{\text{rms}} = \tau_{\text{FWHM}} / (2\sqrt{2 \log(2)}) = 2.76$ ns.

Fig. 3 shows the numerically calculated RMS width τ_{rms} of the output pulse propagating through optimized and un-optimized slow-light and fast-light media as the delay or advancement increases. For the slow light configuration, the un-optimized gain profile is a single Lorentzian gain line [see the blue dashed line in Fig. 3(a)]. Since the signal spectrum is broader than the width of a single gain line, the pulse becomes significantly broadened as the delay increases. At the largest delay of 5.29 ns (a fractional delay of 0.82), the RMS width of the output pulse through our optimized slow-light medium is approximately 3.6 ns while a single-gain-line medium results in a RMS width of 11.5 ns. For the fast-light operation, the un-optimized gain profile is two Lorentzian gain lines separated by 206 MHz [see the red dashed line in Fig. 3(c)]. When the advancement is small, the RMS width of the output pulse through the un-optimized medium is approximately the same as the optimized medium. However, as the advancement becomes large, the noise amplified by the two gain peaks quickly distorts the output pulse for the un-optimized medium while the RMS width of the output pulse through the optimized medium is still well maintained. Note that this calculation assumes that the input pulse is noiseless. In a real experiment, the noise components at the two gain peaks can get amplified much faster, which leads to further distortion of the output pulse.

The modulated pump profile is amplified using an erbium-doped fiber amplifier (EDFA 3 in Fig. 1) and launched into 4 km of SMF counter-propagating with the signal field. A variable optical attenuator (VOA) is used right before the output of the module [15], and the VOA is set at constant output power mode to keep the output power at a fixed level. The amount of delay or advancement is adjusted by controlling the output power level of EDFA 3. Figs. 2(a) and (c) show the measured small signal gain for the fast- and slow-light configurations, respectively. One sees that the optimized flattened gain feature and the transparent window are adequately broad for the signal spectrum shown as the dotted lines. Figs. 2(b) and (d) show the corresponding refractive index change calculated according to the Kramers–Kronig relations. One

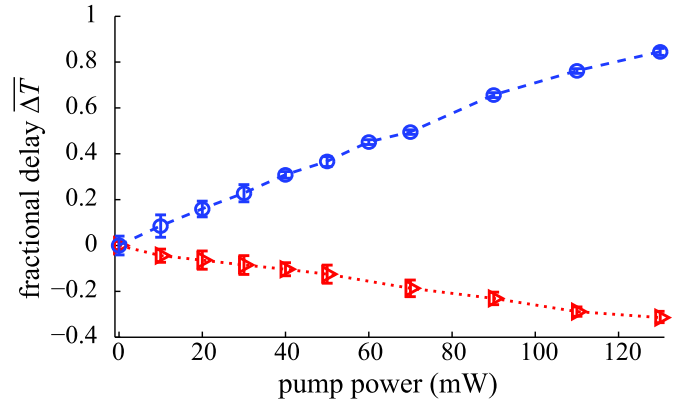


Fig. 4. (Color online.) Measured fractional delay (circles) and advancement (triangles) as functions of the pump power. The error bars are the standard deviations.

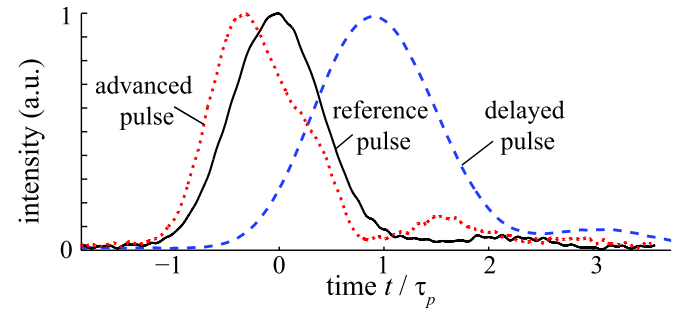


Fig. 5. (Color online.) Output pulse as a function of time for reference, slow-light, and fast-light configurations.

clearly sees the slow- and fast-light regimes, indicated by positive and negative slopes of n , in the vicinity of the center frequency for the two respective configurations. Note that the two chosen gain profiles and their corresponding group index profiles for slow- and fast-light operations are quite uniform over our signal bandwidth, and therefore one can achieve large fractional delay and advancement with very low pulse distortion.

Fig. 4 shows the measured delay and advancement as functions of the pump power. Using a maximum pump power of 130 mW, we have achieved a fractional delay and a fractional advancement of 0.82 and 0.31, respectively, giving a total continuous tuning range of 1.13 pulse width, or about 7.35 ns for 6.5-ns pulses. Note that our setup can switch between slow- and fast-light regimes electronically without the need of rearranging the components. The FWHM of the delayed and advanced pulses are approximately 8.7 ns and 6.7 ns, respectively (see Fig. 5). Note that we do not use the RMS width of the experimentally measured pulse because, in the presence of optical and detector noise, the value of τ_{rms} does not converge as the size of the truncated time window increases, and therefore it no longer reflects accurately the width of the pulses. The fractional advancement can be further improved if each of the double gain features is broadened further and the noise level of the input signal is reduced.

4. Conclusion

In summary, we have demonstrated a single, continuously tunable, low-distortion module for delaying or advancing optical pulses using stimulated Brillouin scattering. The slow- or fast-light operation is realized using dual-stage intensity modulation, with different optimized modulation functions, on the pump field. We have continuously tuned the temporal position of 6.5 ns FWHM Gaussian pulses from a fractional advancement of 0.31 to a frac-

tional delay of 0.82, giving a total tuning range of more than one pulse width, while the pulse distortion is kept low through out the entire tuning range. Such a device can be used for jitter correction and data resynchronization.

Acknowledgements

This work was supported by the DARPA/DSO Slow Light program and by the NSF. The authors acknowledge valuable discussions with Dr. Daniel J. Gauthier and Dr. Alan E. Willner.

References

- [1] R.W. Boyd, D.J. Gauthier, "Slow" and "fast" light, in: E. Wolf (Ed.), in: *Progress in Optics*, vol. 43, Elsevier Science, Amsterdam, 2002, pp. 497–530.
- [2] P. Ku, C. Chang-Hasnain, S. Chuang, *Electron. Lett.* 38 (2002) 1581.
- [3] A. Schweinsberg, N.N. Lepeshkin, M.S. Bigelow, R.W. Boyd, S. Jarabo, *Europhys. Lett.* 73 (2) (2006) 218.
- [4] E. Shumakher, A. Willinger, R. Blit, D. Dahan, G. Eisenstein, *Opt. Express* 14 (19) (2006) 8540.
- [5] Y. Okawachi, J.E. Sharping, C. Xu, A.L. Gaeta, *Opt. Express* 14 (25) (2006) 12022.
- [6] Y. Okawachi, M.S. Bigelow, J.E. Sharping, Z. Zhu, A. Schweinsberg, D.J. Gauthier, R.W. Boyd, A.L. Gaeta, *Phys. Rev. Lett.* 94 (15) (2005) 153902.
- [7] M. González-Herráez, K.Y. Song, L. Thévenaz, *Appl. Phys. Lett.* 87 (2005) 081113.
- [8] Z. Zhu, A.M.C. Dawes, D.J. Gauthier, L. Zhang, A.E. Willner, *J. Lightwave Technol.* 25 (1) (2007) 201.
- [9] K.Y. Song, K. Hotate, *Opt. Lett.* 32 (3) (2007) 217.
- [10] T. Schneider, M. Junker, K.-U. Lauterbach, *Opt. Express* 14 (23) (2006) 11082.
- [11] A. Zadok, A. Eyal, M. Tur, *J. Lightwave Technol.* 25 (8) (2007) 2168.
- [12] R.W. Boyd, D.J. Gauthier, A.L. Gaeta, A.E. Willner, *Phys. Rev. A* 71 (2) (2005) 023801.
- [13] M.D. Stenner, M.A. Neifeld, Z. Zhu, A.M. Dawes, D.J. Gauthier, *Opt. Express* 13 (25) (2005) 9995.
- [14] A. Minardo, R. Bernini, L. Zeni, *Opt. Express* 14 (13) (2006) 5866.
- [15] Z. Shi, R. Pant, Z. Zhu, M.D. Stenner, M.A. Neifeld, D.J. Gauthier, R.W. Boyd, *Opt. Lett.* 32 (14) (2007) 1986.
- [16] Z. Lu, Y. Dong, Q. Li, *Opt. Express* 15 (4) (2007) 1871.
- [17] T. Sakamoto, T. Yamamoto, K. Shiraki, T. Kurashima, *Opt. Express* 16 (11) (2008) 8026.
- [18] M. Lee, R. Pant, M.D. Stenner, M.A. Neifeld, *Opt. Commun.* 281 (10) (2008) 2975.
- [19] K.Y. Song, M.G. Herráez, L. Thévenaz, *Opt. Express* 13 (24) (2005) 9758.
- [20] S. Chin, M. González-Herráez, L. Thévenaz, *Opt. Express* 15 (17) (2007) 10814.
- [21] S. Chin, M. González-Herráez, L. Thévenaz, *Opt. Express* 16 (16) (2008) 12181.
- [22] V.P. Kalosha, L. Chen, X. Bao, *Opt. Express* 14 (26) (2006) 12693.
- [23] R. Tucker, P. Ku, C. Chang-Hasnain, *Electron. Lett.* 41 (4) (2005) 208.
- [24] R.W. Boyd, P. Narum, *J. Mod. Opt.* 54 (16-17) (2007) 2403.
- [25] R. Pant, M.D. Stenner, M.A. Neifeld, Z. Shi, R.W. Boyd, D.J. Gauthier, *Appl. Opt.* 46 (26) (2007) 6513.
- [26] E. Cabrera-Granado, O.G. Calderón, S. Melle, D.J. Gauthier, *Opt. Express* 16 (20) (2008) 16032.
- [27] G.P. Agrawal, *Fiber-Optic Communication Systems*, 3rd edition, Wiley, New York, 2002, Ch. 4.